Protein Science (1998), 7:1976–1982. Cambridge University Press. Printed in the USA.

The structure of serine hydroxymethyltransferase as modeled by homology and validated by site-directed mutagenesis

STEFANO PASCARELLA, SEBASTIANA ANGELACCIO, ROBERTO CONTESTABILE, SONIA DELLE FRATTE, MARTINO DI SALVO, AND FRANCESCO BOSSA

Dipartimento di Scienze Biochimiche "A. Rossi Fanelli" and Centro di Biologia Molecolare del CNR, Università La Sapienza, Roma, Italy

(RECEIVED December 22, 1997; ACCEPTED May 18, 1998)

Abstract

We describe a model for the three-dimensional structure of *E. coli* serine hydroxymethyltransferase based on its sequence homology with other PLP enzymes of the α-family and whose tertiary structures are known. The model suggests that certain amino acid residues at the putative active site of the enzyme can adopt specific roles in the catalytic mechanism. These proposals were supported by analysis of the properties of a number of site-directed mutants. New active site features are also proposed for further experimental testing.

Keywords: aspartate aminotransferase; catalysis; evolution; homology modeling; profile analysis; pyridoxal phosphate; serine hydroxymethyltransferase; site-directed mutagenesis

Serine hydroxymethyltransferase (SHMT: E.C. 2.1.2.1) catalyzes the reversible conversion of serine and tetrahydropteroyglutamate (H_4PteGlu) to glycine and 5,10-methylene-H_4PteGlu (Schirch, 1982). This reaction is the major source of one-carbon groups required in the biosynthesis of methionine, choline, thymidylate, and purines. The SHMT enzyme is widely distributed in nature, and found in both prokaryotic and eukaryotic cells with the latter containing both cytosolic and mitochondrial forms. In addition to H_4PteGlu, the enzyme also requires pyridoxal 5′-phosphate (PLP) as a coenzyme. It is one of a group of PLP enzymes that cleave one of the bonds at the α-carbon of their amino acid substrate. These are referred to as the α-family of PLP enzymes and include the transaminases and amino acid decarboxylases (Alexander et al., 1994).

Three-dimensional structures have been determined for several members of the α-family of vitamin B_6-dependent enzymes. Amongst them are aspartate aminotransferase (AAT; McPhalen et al., 1992; Okamoto et al., 1994; Malashkevich et al., 1995), tyrosine phenol-lyase (1TPL) (Antson et al., 1993), ω-amino acid aminotransferase (Watanabe et al., 1989), 2,2-dialkylglycine decarboxylase (2DKB) (Toney et al., 1995), ornithine aminotransferase (Shen et al., 1994), glutamate-1-semialdehyde aminomutase (Henning et al., 1997), and ornithine decarboxylase (1ORD) (Momany et al., 1995a). Despite the widely differing reaction specificity and weak sequence similarity, these proteins share the same basic folding pattern, which was assumed also for SHMT (Pascarella et al., 1993). The prolonged unavailability of the SHMT atomic structure prompted the construction of a three-dimensional "homology" model that integrated knowledge regarding the enzyme acquired through site-directed mutagenesis experiments and other experimental measures. *Escherichia coli* SHMT was modeled because experimental data are readily available for this enzyme. New features of the active site are proposed for further experimental testing.

Reprint requests to: Francesco Bossa, Dipartimento di Scienze Biochimiche, Università La Sapienza, P. le A. Moro, 5, 00185 Roma, Italy; e-mail: BOSSA@axrma.uniroma1.it.

Results and discussion

Homology modeling was based on the multiple sequence alignment displayed in Figure 1.

Comparison between the C_α main-chain traces of the final *E. coli* SHMT model and the mitochondrial chicken aspartate aminotransferase (7AAT) is reported in Figure 2. They differ mostly in the small domain that was modeled primarily on the 2,2-dialkylglycine decarboxylase structure because of higher local sequence similarity, and better structural compatibility between the SHMT target sequence and the template conformation. The SHMT segment encompassed by positions 369 and 387 was excluded from the model. It is presumably located at the interface between the small and the large domains and may take part in the subunit interface. The proline-rich segment 214–218 is predicted to fold in a nearly extended conformation and connects two β-strands in the PLP binding domain. It occurs in a space region where both an

Fig. 1. Alignment of five structural templates and the *E. coli* (shmt in the figure) sequences reported with the one-letter amino acid code. In each block, top and bottom lines show the numbering of AAT and SHMT sequences, respectively. Dashes represent sequence insertions or deletions. Italic letters in SHMT denote sequence portions excluded from the model. SHMT residues discussed in the text and relevant positions in the structural template sequences are boldfaced. Sequences of the five structural template are reported only from the equivalent N-terminal portion positions and are labelled by their PDB codes (7aat, 2cst, 1ars denote chicken mitochondrial, cytosolic, and *E. coli* aspartate aminotransferases; 2dkb and 1tpl correspond to 2,2-dialkylglycine decarboxylase and tyrosine phenol-lyase respectively).

α-helix in AATs and tyrosine phenol lyase, and an aperiodic structure in dialkylglycine decarboxylase are observed.

Geometrical properties of the model were evaluated by PROCHECK (Laskowski et al., 1993) and were within the accepted ranges. The three-dimensional profile method (Lüthy et al., 1992) indicated that the score calculated for most of the model structure was consistent and comparable with that calculated for the *E. coli* aspartate aminotransferase structure (1ARS), except around sequence position 300 in the small domain, which is at the interface with the large domain. The low score is caused by the occurrence of a few hydrophobic residues at exposed sites, which could be a symptom of local misfolding. The *E. coli* SHMT exists as a dimer at physiological conditions; however, since the deleted segment 369–387 is likely to be involved, no subunit interactions were modeled.

Despite the low sequence similarity amongst many PLP enzymes of the α family with known three-dimensional structure, the basic architecture and conformation of the PLP-binding motif that forms most of the active site is conserved. The motif includes buried β-strands connected by α-helices; the strands' geometry is more conserved to satisfy tighter structural constraints. The comparison of the least similar proteins amongst the five structural templates shows that the largest variations of the relative orientation and dimension of the secondary structure elements are in the small domain. At the low level of sequence similarity between SHMT and the template structures, sequence alignments can become unreliable (Vogt et al., 1995). We used residues Asp200 and Lys229 in the active site region as anchor points for equivalent residues in AAT as well as match optimization of various sequence and structural features. Likewise, the Arg363 was known to correspond to Arg386 in AAT (Delle Fratte et al., 1994). For these reasons, the alignment of the active site region provides a reasonable starting point for homology modeling. The final model confirmed the compatibility of the SHMT sequence with the AAT fold. This conclusion is reinforced by the result of a TOPITS application (Rost et al., 1997) with *E. coli* SHMT as query sequence, where structural compatibility was detected with dialkylglycine decarboxylase and aspartate aminotransferase. This method searches the PDB known structures to assess the correlation between predicted secondary structure and side-chain accessibilities of a query sequence and those observed in all the PDB structures. Each comparison is assigned a score indicative of the quality of the match and is ranked accordingly. In our case, the top scoring structure was dialkylglycine decarboxylase followed by aspartate aminotransferase, with *Z*-scores of 2.83 and 2.77, respectively.

The validity of the active pocket model was also assessed by reconsideration of site directed mutagenesis experiments performed in these, and other, laboratories (Table 1). The substitution of Asp200 reduces the activity of the enzyme to such a level as to prevent any significant characterization of catalytic constants (unpubl. results). The sequence alignment and the structural model (Fig. 3) confirm that Asp200 is structurally equivalent to the identically conserved AAT Asp222 (Mehta et al., 1993), which inter-

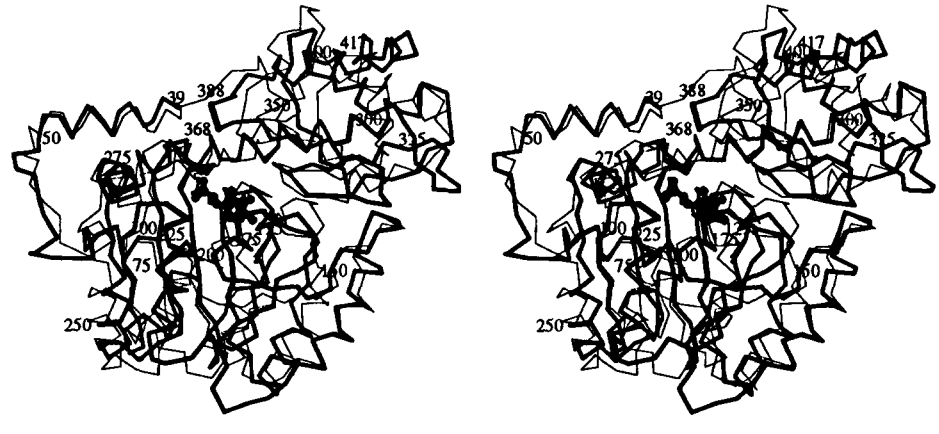

Fig. 2. Superposition of the C_α traces for the monomer SHMT model (thick line) and 7AAT (thin line). The active site PLP is represented by a ball-and-stick model. The thick bond between SHMT site 368–388 indicates the position of the deleted segment. Numbering is shown for C_α atoms at position multiples of 25 except for the N- and C-terminus (positions 39 and 417, respectively).

Table 1. *Mutant forms of E. coli SHMT derived from site-directed mutagenesis experiments*

Mutants[a]	Structural and functional characteristics	References
D200N, D200E, D200A	No catalytic activity with L-serine and allothreonine. D200N and D200E show very slow transamination of D-alanine.	Unpubl. data
A202G	Some significant changes in kinetic and spectral properties compared to wild-type and a lower affinity for PLP.	Unpubl. data
T226A	Normal affinity for substrates and coenzymes but only 3% of the catalytic activity of wild-type. T226 plays an important role in converting the gem-diamine complex to the external aldimine complex and for determining substrate specificity.	Angelaccio et al. (1992)
H228N, H228D	k_{cat} for the mutant enzymes about 25% of the values for the wild-type enzyme with either L-serine or allothreonine as substrates; K_m for amino acid substrates and reduced folate compounds are 2–20-fold larger than those for wild-type. H228N and H228D mutants catalyze the transamination of D-alanine at approximately the same rate as the wild-type while H228D transaminates L-alanine by an order of magnitude faster than H228N and wild-type SHMTs.	Hopkins and Schirch (1986) Stover et al. (1992)
K229H, K229Q, K229R	Significant differences in spectral properties of K229H and K229R relative to wild-type. Both K229H and K229R do not show catalytic activity with L-serine and allothreonine; no transamination of D-alanine was observed. K229Q could catalyze one turnover of either serine to glycine or glycine to serine at rates approaching those of the wild-type enzyme. After one turnover, K229Q could not expel the product and could not bind new substrate while it could transaminate D-alanine.	Schirch et al. (1993) Iurescia et al. (1996)
R235D, R235Q	Same results as for D200A	Unpubl. data
R363A, R363K	R363A does not bind serine and glycine and shows no activity with serine as substrate. R363K exhibits only 0.03% of the catalytic activity of the wild-type enzyme and a 15-fold reduction in affinity for glycine and serine. Both the mutant enzymes bind amino acid esters at the active site.	Delle Fratte et al. (1994)

[a] Amino acids indicated by one-letter code.

acts with the pyridine nitrogen and stabilizes its positive charge (Kirsch et al., 1984; Yano et al., 1992). Ala202 is also strictly conserved and occurs at an equivalent position in AATs and other PLP-dependent enzymes of the α-family. According to the model, this residue contributes to the correct positioning of the PLP at the active site, where a smaller or larger side chain would perturb the geometry of the cofactor binding site. Experimental results indicate that the SHMT mutant Ala202Gly shows a fivefold lower k_{cat} for allothreonine and a 50% lowered affinity for PLP (R. Contestabile & S. Angelaccio, unpubl. data). Each of five threonine residues (224, 225, 226, 227, and 230) near the active site lysyl residue (Lys229) were alternatively mutated to alanine (Angelaccio et al., 1992). Of these, Thr226, 227, and 230 are either conserved, or substituted by serines in the 32 available SHMT sequences. Thr226 is the only site where mutations induce significant activity modifications (Table 1). According to the model (Fig. 4), Thr226 can form an H-bond to the εNH_2 of the Lys229 in the external aldimine or to one of the oxygens of the PLP phosphate group (Angelaccio et al., 1992). This role is reminiscent of that of AAT Tyr70 (Kirsch et al., 1984; Hayashi & Kagamiyama, 1995), which may correspond to the nonconserved SHMT Tyr59. Thr226 is equivalent to AAT Ser255, a position at which many enzymes of the α-family bear an hydroxyl group. Lack of the SHMT dimeric model hampers a better understanding of the role of Thr226. Thr224, 225, 227, and 230, however, are not within interacting distance of the active site and are relatively insensitive to mutations (Angelaccio et al., 1992). His228 occurs in a position compatible with its observed catalytic role, such that it can interact with the hydroxyl group of the serine side chain in the external aldimine (Fig. 4) at a distance of about 3.0 Å, in agreement with experimental results (Stover et al., 1992). Arg235 corresponds to AAT Arg266, which forms two H-bonds with the 5′-phosphate ester group of the coenzyme. The model suggests that this residue, conserved in all SHMTs with the exception of enzymes from *Methanococcus jannaschii* (Swiss-Prot code glya_metja) and *Methanobacterium thermoautotrophicum* (glya_metth) where it is replaced by a glutamine, plays a similar role. Arg235 is a critical residue since its substitution dramatically decreases the enzyme activity with L-serine and allothreonine as substrates (Table 1). Arg363 is also positioned to interact with the α-carboxylate of the amino acid substrate as clearly demonstrated by mutagenesis experiments (Delle Fratte et al., 1994). Interaction between α-carboxylate group of serine substrate and guanidinium group of Arg363 fixes the conformation of the external aldimine (Fig. 4) in such a way that the C_α-C_β bond to be cleaved is nearly perpendicular to the pyridine ring, consistently with hypothesis (Dunathan, 1966). The model

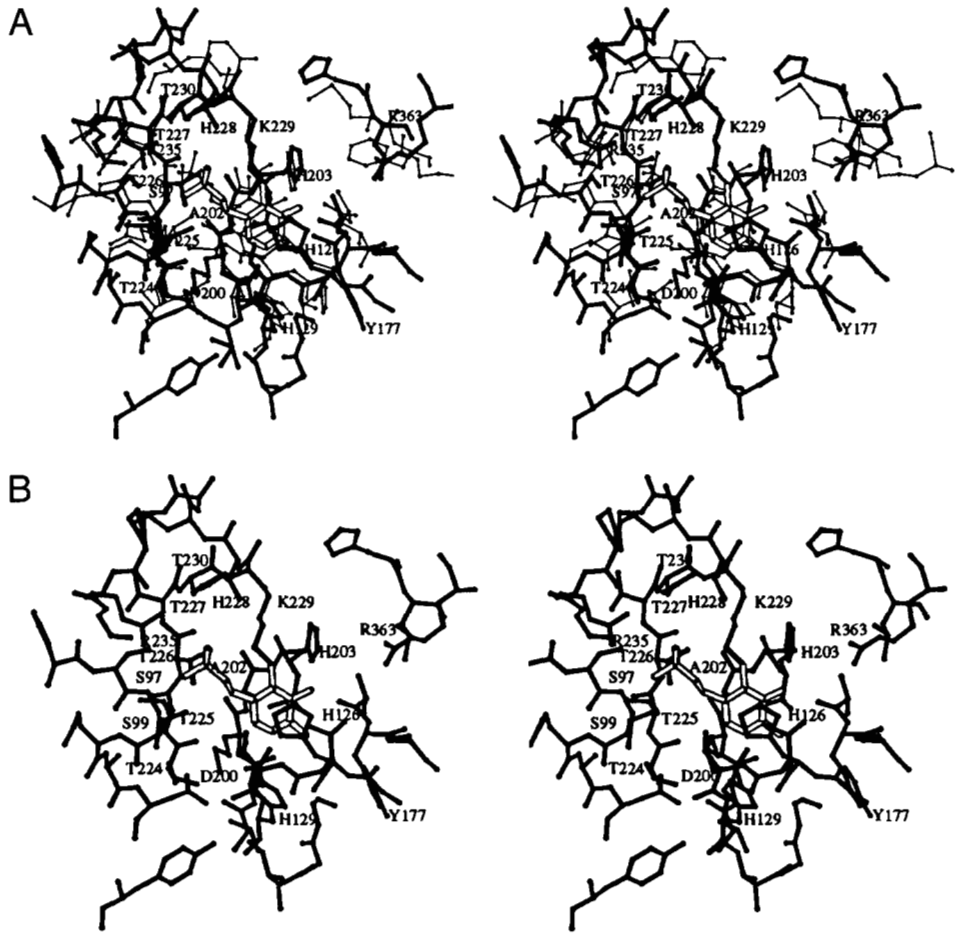

Fig. 3. (**A**) Superposition between SHMT (thick lines) and 7AAT (thin) active sites and (**B**) the SHMT active site. PLP is represented as open bonds. Residues are labeled by the one-letter code and by sequence position.

also explains the stereochemical study (Malthouse et al., 1991), which showed that the enzymes catalyze the exchange of the pro-2S proton of glycine, which is stereochemically equivalent of hydroxyl group of serine, 7,400 times faster than the pro-2R proton. Cys410 is predicted to be exposed and far from the active site, in agreement with earlier results (Joshi-Tope & Schirch, 1990).

The analysis of the SHMT active site, combined with evolutionary considerations, highlights further conserved or conservatively substituted residues that occur in positions suggestive of a catalytic or structural function and which can be tested by site-directed mutagenesis. Ser97 is conserved and predicted to form an H-bond to the phosphate group of PLP (Fig. 3). It is also present in several AATs with a similar role, and probably it is utilized to correctly position the phosphate group of PLP. Gly98 is also identically conserved and aids in forming the binding site for the PLP phosphate. The structurally equivalent Gly108 in AATs is also conserved and occurs in a position where no C_β could be tolerated due to steric hindrance with the PLP phosphate. Ser99 is found in many SHMTs and predicted by the model to interact with the same phosphate group. It is matched to the AAT Thr109, which is generally conserved with exception of *Sulfolobus solfataricus* where a lysyl residue is found instead. His126 is nearly parallel to the PLP ring and it is modeled to form an H-bond to Thr128. The former is strictly conserved while the latter is conservatively replaced by Ser. The two residues are structurally equivalent to the conserved AAT Trp140 and Asn142, respectively. His129 in SHMT can interact with Asp200 and the N1 of the PLP ring and it is equivalent to the conserved His143 of AATs. This latter residue was replaced with Ala and Asn in AAT (Yano et al., 1991) by site-directed mutagenesis, and the results suggested that, although it is not essential for catalysis, it may well assist the formation of the enzyme-substrate complex. A site-directed mutagenesis study on three His residues of the sheep cytosolic SHMT was recently reported (Jagath et al., 1997), two of which correspond to *E. coli* His126 and His129. The role observed for the former is consistent with the model, namely, it interacts with PLP. However, experimental evidence presented (Jagath et al., 1997) would suggest that the latter His residue may be the base responsible for abstraction the α-proton from the substrate. This apparently conflicts with the role predicted by the model for the same residue. His203 can interact with the PLP phenolate and should be structurally equivalent to the conserved AAT Tyr225 (Goldberg et al., 1991).

The structure of ornithine decarboxylase (1ORD) (Momany et al., 1995a) was not included in the set of template structures. However, only one of its five domains is clearly structurally homologous to the PLP-binding domain in AATs. A similarity between the active site sequence of SHMT and other decarboxylases has already been described (Bossa et al., 1976) including, for

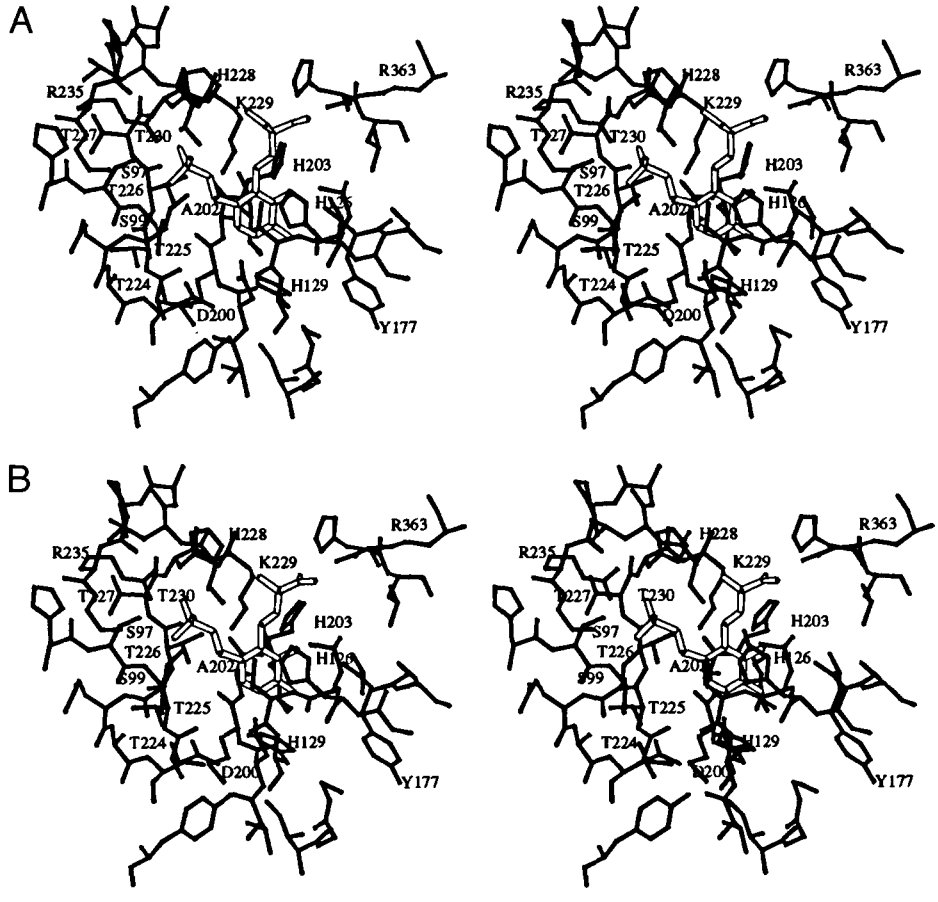

Fig. 4. Active site SHMT model for external aldimines of (**A**) serine and (**B**) D-alanine. PLP is represented by open bonds. Residues are labeled by the one-letter code and by sequence position.

example, His228 (354 in 1ORD). Comparison between the sequences and structures of 1ORD and SHMT indicates other common residues like His126 (223 in 1ORD). SHMT Gly179 might be matched to 1ORD Gly294 and to the conserved AAT Gly197 by a slight modification of the alignment in Figure 1. This latter residue belongs to a conserved segment (AAT positions 193–197) at the large/small domain interface, and is not at interacting distance from the active site. SHMT Gly179 is not conserved (replaced by Arg, Phe, Gln) and therefore no evidence supports its equivalence to a functionally important residue. Structural comparison between the SHMT and 1ORD active sites shows that the model largely converges to the decarboxylase structure. For example, His126 and 1ORD His223 share a similar geometry relative to the cofactor ring. Conformation of PLP at both active sites reflects the differences of cofactor binding between 1ORD and AATs, especially at its phosphate moiety. Consequently, a major deviation is observed between side-chain conformation of SHMT His228 and decarboxylase His354. This latter residue is proposed to interact with the cofactor phosphate, mainly to replace the function of AAT Arg266, which is absent in decarboxylases (Momany et al., 1995b). The presence of Arg235 in SHMT, equivalent to AAT Arg266, and, above all, experimental evidence (Stover et al., 1992) suggest that His228 can interact with the hydroxymethyl group of the substrate serine. The different conformation can thus be justified by the diverse roles that these His residues can play in SHMTs and prokaryotic decarboxylases. The PLP binding site differs also at decarboxylase Ser197, equivalent to the conserved AAT Gly108 and SHMT Gly98. To assess the impact of the 1ORD coordinates onto the final SHMT model, we used the InsightII module Modeller, which implements the modeling method (Šali & Blundell, 1993) based on satisfaction of spatial restraints derived from structural templates. To avoid overrepresentation of AATs, we included in the template set only 7AAT, 2DKB, and the PLP-binding domain of 1ORD aligned according to Figure 1 and to previous analysis (Momany et al., 1995b). Comparison between the original and ten new SHMT active site models built with Modeller showed overall structural convergence. Conformation of His228 side chain was less defined due to the predicted occupation of two different rotameric states, one of which corresponds to that assumed in the original model on the basis of experimental evidence (Stover et al., 1992).

We built a model of the external aldimine with D-ala (Fig. 4) to propose possible explanations of the racemization and transamination activity observed for SHMT (Shostak & Schirch, 1988). Experimental evidence suggested the presence of two bases at the opposite sides of the PLP ring as a requirement for correct stereochemistry of racemization (Shostak & Schirch, 1988). The model shows at least two active site His residues (SHMT sites 126 and 203 in Fig. 4) with approximately appropriate positions to act as the expected bases. It must be noted, however, that the distances between the atoms εN of His126 and 203 and C_α of the substrate

are about 4.2 and 4.5 Å, respectively. The long distance can be explained by model inaccuracy and/or by the lack of an appropriate simulation of the transition between open-closed form, which could influence the relative position of PLP and nearby side chains, similar to that observed in AATs (Kirsch et al., 1984). We assumed a cofactor tilt of about 20° and a rotation of His126 of about 30° around C_β-C_γ bond upon substrate binding.

The analysis of the modeled active site has thus suggested several residues, among the many identically conserved in the 32 SHMT sequences, that are good candidates for rational site-directed mutagenesis experiments, and has also provided a framework for the interpretation of the properties of mutant enzymes produced in the past decade. Nonetheless, many features of the SHMT structure and activity remain obscure, especially the interaction of the second substrate H_4PteGlu at the active site and the geometry of the dimer interface. However, the presence of several charged or polar side chains, such as histidines, in the modeled active site provide a structural basis for the catalytic versatility of SHMT. This enzyme displays transaminase, decarboxylase, and racemase activities associated with other PLP-dependent enzymes (Schirch, 1982). However, as in AATs, a few residues could contribute to the construction of the active site from the adjacent subunit, and this could account for some properties of the enzyme, which cannot be explained by our model. Given the protracted absence of the crystallographic structure, the model presented here provides the only tertiary framework from which to continue structural work, to unravel the structure of the physiological dimer, and also to elucidate further details of the active site, interaction with H_4PteGlu, and other catalytic events. Comparison of the theoretical SHMT model with the experimentally determined structure will help in assessing the accuracy of homology modeling techniques applied at low level of similarity between target and template sequences. Coordinates of the model are available at URL http://bach.bio.uniroma1.it/SHMT.

Materials and methods

Thirty-two SHMT isoenzyme sequences from various sources extracted from the Swiss-Prot databank (Bairoch & Boeckmann, 1991) were aligned with the GCG routine "Pileup" (Wisconsin Package Version 9.0, Genetics Computer Group, Madison, Wisconsin). The resulting multiple alignment was utilized for secondary structure prediction and for detection of evolutionarily conserved residues.

The homology model of *E. coli* SHMT was based on the structures of five PLP-dependent enzymes: mitochondrial (McPhalen et al., 1992) and cytosolic (Malashkevich et al., 1995) chicken aspartate aminotransferases (PDB codes 7AAT and 2CST, respectively), *E. coli* (Okamoto et al., 1994) aspartate aminotransferase (1ARS), tyrosine phenol lyase (Antson et al., 1993) from *Citrobacter intermedius* (1TPL), and dialkylglycine decarboxylase (Toney et al., 1995) from *Pseudomonas cepacia* (2DKB). Despite the low sequence similarity among the templates and the target enzyme (15% identity on average), they are considered structurally homologous on the basis of several theoretical (Mehta et al., 1993; Pascarella et al., 1993) and experimental considerations (Schirch, 1982).

The preliminary step in any homology modeling approach is the construction of an accurate sequence alignment among the template structures and the target sequence, which is difficult in cases of low sequence similarity. Each of the four templates (2CST, 1ARS, 1TPL, and 2DKB) were individually superposed on the 7AAT structure using C_α carbon atom coordinates for which technical details are available (Rossmann & Argos, 1975). The combined superpositions were manually inspected and refined, and a multiple sequence alignment subsequently derived from the resulting structural equivalencies. A profile (Gribskov et al., 1987) was calculated from this alignment and the target *E. coli* SHMT sequence matched to it using the GCG program "Profilegap." Statistical significance of the sequence similarity between the *E. coli* SHMT sequence and the profile derived from the other PLP enzymes is discussed elsewhere (Pascarella et al., 1993). However, due to the overall low sequence similarity, the resulting alignment was manually refined to optimize the matching of several characteristics including (a) observed and predicted secondary structures, (b) conserved SHMT hydrophobic side chains and buried positions in the template structures, (c) functionally important sites such as the PLP-binding active site lysine, and (d) insertions/deletions. The alignment and superposition of the five structures showed that the common fold began at Thr39 of the *E. coli* SHMT sequence (Fig. 1). After deletion of the 38-residue N-terminus and of the segment Ile369–Cys387 (Fig. 1), because they are not homologous to the structural templates, our model contained 360 residues (86.0% of the entire sequence). However, part of the latter C-terminal segment is predicted to fold with an α-helical conformation and contains the potentially important Arg372 conserved in most SHMTs.

Molecular modeling utilized the packages Homology and Discover in Insight (InsightII user guide, October 1995, Biosym/MSI, San Diego, California). Structurally conserved regions (SCR) were identified on the multiple structure superposition (Greer, 1981) and coordinates were correspondingly assigned to the target SHMT sequence. The conformation of the side chains was also modeled as close as possible to that of the corresponding residues in the structural templates. Nonconserved regions were modeled by selecting the structure among the five templates, which best adapted to the target structural environment. The loops connecting the SCR were modeled using the function "search_loop" implemented in Insight, which searches a set of selected Protein Data Bank (Bernstein et al., 1977) structures for loops that best fit the given structural environment. The coordinates for the SHMT segment PNPVP (positions 214–218 with one-letter sequence code) were taken from the fragment PRPLP at positions 224–228 of chain C of thymidylate synthase structure (PDB code 2TSC). This structure fragment was selected by searching the NRL_3D databank (Pattabiraman et al., 1990) with the GCG routine "Findpattern" and PXPXP as the query pattern (X meaning any residue).

Side chain conformations were manually refined and the most severe steric overlaps removed. Several cycles of constrained energy minimization regularized the structure and relative geometrical parameters. Geometrical and local environmental consistency of the model were checked with the programs Procheck (Laskowski et al., 1993) and Profile3D (Lüthy et al., 1992). Hydrogen bonds were analyzed with the program Hbplus (McDonald & Thornton, 1994). Secondary structure predictions were calculated from the Phd server (Rost & Sander, 1994). Stereo pictures were produced by the program Molscript (Kraulis, 1991).

Acknowledgments

This work was funded in part by CNR grants n. 94.00404.12, n. 95.00434.12, n.96.03828.12 and CNR Strategic project on Structural Biology. Authors are grateful to Prof. Verne Schirch and Prof. Patrick Argos for manuscript revision and helpful discussion. Authors wish also to thank the anonymous referees who gave valuable suggestions to improve the manuscript.

References

Alexander F, Sandmeier E, Mehta PK, Christen P. 1994. Evolutionary relationship among pyridoxal-5′-phosphate-dependent enzymes. Regio-specific α, β and γ families. *Eur J Biochem 219*:953–960.

Angelaccio S, Pascarella S, Fattori E, Bossa F, Strong W, Schirch V. 1992. Serine hydroxymethyltransferase: Origin of substrate specificity. *Biochemistry 31*:155–162.

Antson AA, Demidkina TV, Gollnick P, Dauter Z, Von Tersch RL, Long J, Berezhnoy SN, Phillips RS, Harutyunyan EH, Wilson KS. 1993. Three-dimensional structure of tyrosine phenol-lyase. *Biochemistry 32*:4195–4206.

Bairoch A, Boeckmann B. 1991. The SWISS-PROT protein sequence data bank. *Nucleic Acids Res 19*:2247–2249.

Bernstein FC, Koetzle TF, Williams GJ, Meyer EE Jr, Brice MD, Rodgers JR, Kennard O, Shimanouchi T, Tasumi M. 1977. The Protein Data Bank: A computer-based archival file for macromolecular structures. *J Mol Biol 112*:535–542.

Bossa F, Barra D, Martini F, Schirch LV, Fasella P. 1976. Serine transhydroxymethylase from rabbit liver. Sequence of a nonapeptide at the pyridoxal-5′-phosphate-binding site. *Eur J Biochem 70*:397–401.

Delle Fratte S, Iurescia S, Angelaccio S, Bossa F, Schirch V. 1994. The function of arginine 363 as the substrate carboxyl-binding site in *Escherichia coli* serine hydroxymethyltransferase. *Eur J Biochem 225*: 395–401.

Dunathan HC. 1966. Conformation and reaction specificity in pyridoxal phosphate enzymes. *Proc Natl Acad Sci USA 55*:712–716.

Goldberg JM, Swanson RV, Goodman HS, Kirsch JF. 1991. The tyrosine-225 to phenilalanine mutation of *Escherichia coli* aspartate aminotransferase results in an alkaline transition in the spectrophotometric and kinetic pK_a values and reduced values of both k_{cat} and K_m. *Biochemistry 30*:305–312.

Greer J. 1981. Comparative model-building of the mammalian serine proteases. *J Mol Biol 153*:1027–1042.

Gribskov M, McLachlan AD, Eisenberg D. 1987. Profile analysis: Detection of distantly related proteins. *Proc Natl Acad Sci USA 84*:4355–4358.

Hayashi H, Kagamiyama H. 1995. Reaction of aspartate aminotransferase with L-erythro-3-hydroxyaspartate: Involvement of Tyr70 in stabilization of the catalytic intermediates. *Biochemistry 34*:9413–9423.

Henning M, Grimm B, Contestabile R, John RA, Jansonius JN. 1997. Crystal structure of glutamate-1-semialdehyde aminomutase: An α_2-dimeric vitamin B_6-dependent enzyme with asymmetry in structure and active site reactivity. *Proc Natl Acad Sci USA 94*:4866–4871.

Hopkins S, Schirch V. 1986. Properties of a serine hydroxymethyltransferase in which an active site histidine has been changed to an asparagine by site-directed mutagenesis. *J Biol Chem 261*:3363–3369.

Iurescia S, Condò I, Angelaccio S, Delle Fratte S, Bossa F. 1996. Site-directed mutagenesis techniques in the study of *Escherichia coli* serine hydroxymethyltransferase. *Protein Expr Purif 7*:323–328.

Jagath JR, Sharma B, Appaji Rao N, Savithri HS. 1997. The role of His-143, -147, and -150 residues in subunit assembly, cofactor binding, and catalysis of sheep liver cytosolic serine hydroxymethyltransferase. *J Biol Chem 272*:24355–24362.

Joshi-Tope G, Schirch V. 1990. The role of a critical sulfhydryl group in the mechanism of serine hydroxymethyltransferase. *Annals NY Acad Sci 585*:339–345.

Kirsch JF, Eichele G, Ford GC, Vincent MG, Jansonius JN, Gehring H, Christen P. 1984. Mechanism of action of aspartate aminotransferase proposed on the basis of its spatial structure. *J Mol Biol 174*:497–525.

Kraulis J. 1991. Molscript: A program to produce both detailed and schematic plots of protein structures. *J Appl Crystallogr 24*:946–950.

Laskowski RA, MacArthur MW, Moss DS, Thornton JM. 1993. PROCHECK: A program to check the stereochemical quality of protein structures. *J Appl Crystallogr 26*:283–291.

Lüthy R, Bowie JU, Eisenberg D. 1992. Assessment of protein models with three-dimensional profiles. *Nature 356*:83–85.

Malthouse JPG, Milne JJ, Gariani LS. 1991. A comparative study of the kinetics and stereochemistry of the serine hydroxymethyltransferase- and tryptophan synthase-catalysed exchange of the pro-2R and pro-2S protins of glycine. *Biochem J 274*:807–812.

Malashkevich VN, Strokopytov BV, Borisov VV, Dauter Z, Wilson KS, Torchinsky YM. 1995. Crystal structure of the closed form of chicken cytosolic aspartate aminotransferase at 1.9 Å resolution. *J Mol Biol 247*:111–124.

McDonald IK, Thornton JM. 1994. Satisfying hydrogen bonding potential in proteins. *J Mol Biol 238*:777–793.

McPhalen CA, Vincent MG, Jansonius JN. 1992. X-ray structure refinement and comparison of three forms of mitochondrial aspartate aminotransferase. *J Mol Biol 225*:495–517.

Mehta PK, Hale TI, Christen P. 1993. Aminotransferases: Demonstration of homology and division into evolutionary subgroups. *Eur J Biochem 214*:549–561.

Momany C, Ernst S, Ghosh R, Chang NL, Hackert ML. 1995a. Crystallographic structure of a PLP-dependent ornithine decarboxylase from *Lactobacillus* 30a to 3.0 Å resolution. *J Mol Biol 252*:643–655.

Momany C, Ghosh R, Hackert ML. 1995b. Structural motifs for pyridoxal-5′-phosphate binding in decarboxylases: An analysis based on the crystal structure of the *Lactobacilus* 30a ornithine decarboxylase. *Protein Sci 4*:849–854

Okamoto A, Higuchi T, Hirotsu K, Kuramitsu S, Kagamiyama H. 1994. X-ray crystallographic study of pyridoxal 5′-phosphate-type aspartate aminotransferase from *Escherichia coli* in open and closed form. *J Biochem 116*:95–107.

Pascarella S, Schirch V, Bossa F. 1993. Similarity between serine hydroxymethyltransferase and other pyridoxal phosphate-dependent enzymes. *FEBS Lett 331*:145–149.

Pattabiraman N, Namboodiri K, Lowrey A, Gaber BP. 1990. NRL_3D: A sequence-structure database derived from the protein data bank (PDB) and searchable within the PIR environment. *Protein Seq Data Anal 3*:387–405.

Rost B, Sander C. 1994. Combining evolutionary information and neural networks to predict protein secondary structure. *Proteins 19*:55–77.

Rost B, Schneider R, Sander C. 1997. Fold recognition by prediction-based threading. *J Mol Biol 270*:1–10.

Rossmann MG, Argos P. 1975. A comparison of the heme binding pocket in globins and cytochrome b_5. *J Biol Chem 250*:7525–7532.

Šali A, Blundell TL. 1993. Comparative protein modelling by statisfaction of spatial restraints. *J Mol Biol 234*:779–815.

Schirch D, Delle Fratte S, Iurescia S, Angelaccio S, Contestabile R, Bossa F, Schirch V. 1993. Function of the active-site lysine in *Escherichia coli* serine hydroxymethyltransferase. *J Biol Chem 268*:23132–23138.

Schirch V. 1982. Serine hydroxymethyltransferase. *Adv Enzymol 53*:83–111.

Shen BW, Ramesh V, Müller R, Hohenester E, Hennig M, Jansonius JN. 1994. Crystallization and preliminary X-ray diffraction studies of recombinant human ornithine aminotransferase. *J Mol Biol 243*:128–130.

Shostak K, Schirch V. 1988. Serine hydroxymethyltransferase: Mechanism of the racemization and transamination of D- and L-alanine. *Biochemistry 27*:8007–8014.

Stover P, Zamora M, Shostak K, Gautam-Basak M, Schirch V. 1992. *Escherichia coli* serine hydroxymethyltransferase: The role of histidine 228 in determining reaction specificity. *J Biol Chem 267*:17679–17687.

Toney MD, Hohenester E, Keller JW, Jansonius JN. 1995. Structural and mechanistic analysis of two refined crystal structures of the pyridoxal phosphate-dependent enzyme dialkylglycine decarboxylase. *J Mol Biol 245*:151–179.

Vogt G, Etzold T, Argos P. 1995. An assessment of amino acid exchange matrices in aligning protein sequences: The twilight zone revisited. *J Mol Biol 249*:816–831.

Watanabe N, Sakabe N, Sakabe K, Higashi T, Sasaki K, Aibara S, Morita Y, Yonoha K, Toyama S, Fukutani H. 1989. Crystal structure analysis of ω-aminoacid: Pyruvate aminotransferase with newly developed Weissenberg camera and an imaging plate using synchrotron radiation. *J Biochem 105*:1–3

Yano T, Kuramitsu S, Tanase S, Morino Y, Hiromi K, Kagamiyama H. 1991. The role of His-143 in the catalytic mechanism of *Escherichia coli* aspartate aminotransferase. *J Biol Chem 266*:6079–6085.

Yano T, Kuramitsu S, Tanase S, Morino Y, Kagamiyama H. 1992. Role of Asp222 in the catalytic mechanism of *Escherichia coli* aspartate aminotransferase: The amino acid residue which enhances the function of the enzyme-bound coenzyme pyridoxal-5′-phosphate. *Biochemistry 31*:5878–5887.